

*Technical Memorandum No. 33-177*

*A Pneumatic Model Launcher for Free-Flight Testing  
in a Conventional Wind Tunnel*

*H. P. Holway*

*J. G. Herrera*

*B. Dayman, Jr.*

GPO PRICE \$ \_\_\_\_\_

OTS PRICE(S) \$ \_\_\_\_\_

Hard copy (HC) 1.00

Microfiche (MF) .50

N 65 17215

(ACCESSION NUMBER)

(PAGES)

(NASA CR OR TMX OR AD NUMBER)

(THRU)

(CODE)

(CATEGORY)



JET PROPULSION LABORATORY  
CALIFORNIA INSTITUTE OF TECHNOLOGY  
PASADENA, CALIFORNIA

July 30, 1964

RQT-26373

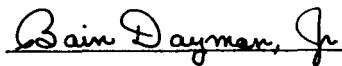
*Technical Memorandum No. 33-177*

*A Pneumatic Model Launcher for Free-Flight Testing  
in a Conventional Wind Tunnel*

*H. P. Holway*

*J. G. Herrera*

*B. Dayman, Jr.*



Bain Dayman, Jr., Chief

Aerodynamic Facilities Section

JET PROPULSION LABORATORY  
CALIFORNIA INSTITUTE OF TECHNOLOGY  
PASADENA, CALIFORNIA

July 30, 1964

Copyright © 1964  
Jet Propulsion Laboratory  
California Institute of Technology

Prepared Under Contract No. NAS 7-100  
National Aeronautics & Space Administration

## CONTENTS

I. Introduction . . . . .	1
II. Design Criteria . . . . .	2
III. General Description of Launching Technique . . . . .	2
IV. Development History and Problems . . . . .	4
V. Future Design Improvements . . . . .	7
VI. Model Construction Techniques . . . . .	8
VII. Moment-of-Inertia and Center-of-Gravity Measurements . . . . .	10
VIII. Approximate Equations of Motion . . . . .	13
IX. Summary . . . . .	13
Nomenclature . . . . .	14
References . . . . .	15

## FIGURES

1. Installation of pneumatic launcher in supersonic facility . . . . .	2
2. High-speed motion pictures of 10-deg half-angle cone model launched at 20-deg angle of attack . . . . .	3
3. Early installation of pneumatic launching assembly . . . . .	4
4. Later developments of launching system, installation in supersonic facility . . . . .	4
5. Installation of launching system with model exposed to airstream . . . . .	4
6. Triangular-shaped blade support for cone models . . . . .	5
7. Components of pneumatic launcher . . . . .	5
8. Bench calibration setup . . . . .	6
9. Plot of velocity vs chamber pressure for launcher . . . . .	7
10. Injection molding press . . . . .	8
11. Model mold of 10-deg half-angle 1.00-in. base diameter cone . . . . .	9



**FIGURES (Cont'd)**

12. Cutaway view of assembled 10-deg half-angle cone model . . . . .	9
13. Instrument for measuring the moment of inertia . . . . .	10
14. Analytical balances for locating the center of gravity . . . . .	11
15. Plot of $I$ vs $t^2$ . . . . .	11
16. Schematic of center-of-gravity measuring system . . . . .	12
17. Plot showing accuracy of center-of-gravity measurements . . . . .	12

**ABSTRACT**

17215

The adoption of ballistic range techniques to a conventional wind tunnel is enhanced through the use of a pneumatic model launcher. The problems encountered during the development are discussed, and the subsequent solutions are presented.

An inexpensive technique for the fabrication of expendable models was developed through the use of polystyrene plastic in the injection-molding process. The precision of the free-flight, support-free aerodynamic data is dependent upon the high degree of accuracy in the measurements of both the moment of inertia and the center of gravity. These measurements were made possible with the development of special instruments, which are explained in the text.

*Butler***I. INTRODUCTION**

The problem of obtaining wind-tunnel aerodynamic data free of support interference has been the topic of discussion for many years. For most typical model installations, the model support (sting) alters the flow field in the base region. For example, the presence of the support may increase the cross-sectional area of the wake and/or change the axial position of the wake neck. In turn, base pressure is affected, thereby altering certain aerodynamic parameters, particularly the chord or drag-force coefficients.

Some time ago, free-flight experiments were initiated in the supersonic and hypersonic wind tunnels at the Jet Propulsion Laboratory (JPL). At first, the models were supported on a thin wire at the upstream end of the viewing area. After breaking the wire, spark schlieren photographs were taken of the near-wake regions of the models in flight. In addition, high-speed motion pictures

were taken of models (released at angle of attack) as they oscillated during their trajectory across the viewing area. From these pictures, various aerodynamic parameters, such as drag, lift, pitching moment, and pitch damping (dynamic stability), were determined. The technique, procedure, and results for these experiments have been reported (Refs. 1, 2 and 3). Since these initial series of free-flight experiments produced high-quality data, many similar experiments followed. It became apparent, however, that it would be advantageous to view the model for a longer period of time during any one flight. Since increasing the existing viewing area was impractical, the concept of using a launch tube to propel models upstream was conceived. In addition to significantly increasing the observable distance of model travel over that obtained with wire-launch technique, it is also possible to place several launch tubes in the tunnel, thereby increasing the number of flights possible in a given time period.

## II. DESIGN CRITERIA

The design criteria for the pneumatic launcher follow: (1) the launcher had to be able to propel the models from a point downstream of the viewing window to just the upstream edge of the window (a distance of approximately 34 in. in the supersonic wind tunnel); (2) the angle of attack ( $\alpha$ ) at release could be set from 0 to 180

deg for both slender models and for short, blunt models; (3) the mass of the models could vary from 3 to 100 g; and (4) since the trajectory is determined by the model shape, mass, and tunnel dynamic pressure, the launch velocities could vary from 20 to 100 ft/sec.

## III. GENERAL DESCRIPTION OF THE LAUNCHING TECHNIQUE

Because of the structural geometry of the supersonic wind tunnel, the pneumatic launcher assembly was mounted 3 in. off the tunnel centerline to the side. In order to compensate for the gravity effect and maintain the model's flight as near centered in the viewing window as possible, the assembly was mounted 2 in. above the tunnel centerline. The release point for the model was 7 in. downstream of the trailing edge of the viewing window. This was done to insure that the wake of the model would be free from any influence of the projecting mechanism. More information regarding the model wake can be found in Ref. 2.

In general, the model is mounted on the launcher at the desired angle of attack and is secured there by a set of holding fingers while tunnel flow conditions are established. An installation of a model at 20-deg angle of attack is shown in Fig. 1. A cam-actuated micro switch coupled to the holding-finger shaft, when operated to open the fingers, also starts a high-speed camera. An event switch, excited at the same time as the camera, actuates the piston release mechanism approximately 0.2 to 0.3 of a second later, starting the model on its way. This delay is necessary to allow for the high-speed camera to come up to the selected speed (5000 frames/sec) before the model appears in the viewing area. The

picture sequence in Fig. 2 shows the flight of a model released at 20-deg angle of attack. As many as nine complete cycles of oscillatory model motion in a given flight have been filmed using this technique.

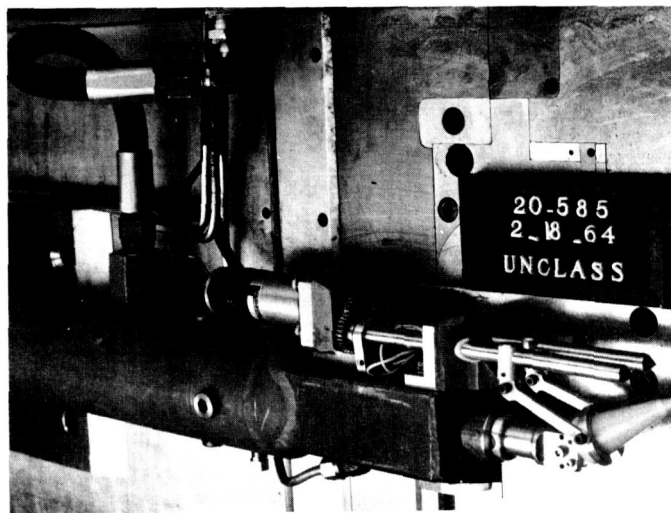
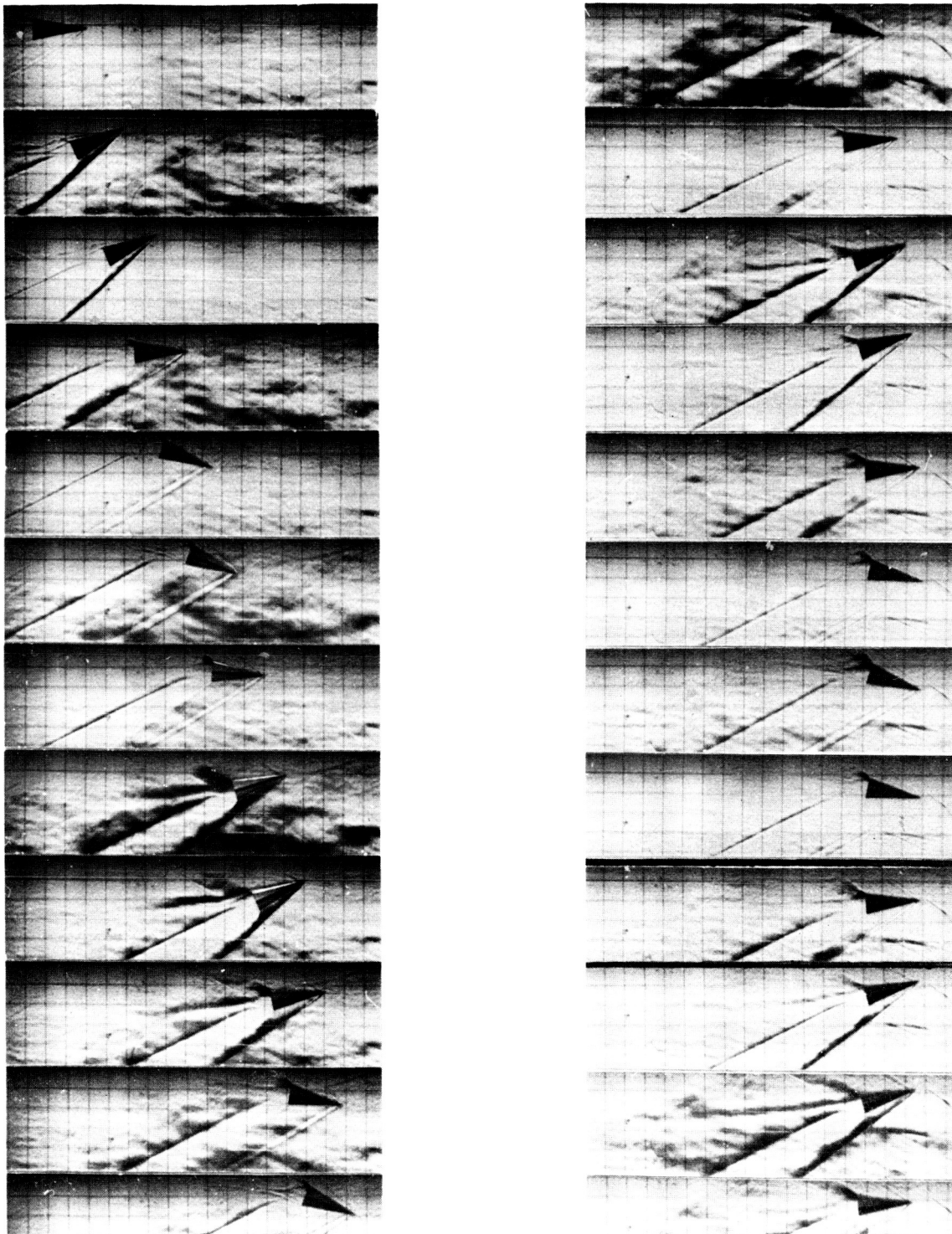


Fig. 1. Installation of pneumatic launcher in supersonic facility



SUPPLY PRESSURE ( $P_s$ ) OF 43.2 cm Hg abs  
 MASS 12.79 g  
 cg = 1.5 in. AFT OF NOSE  
 MACH NUMBER 2.01

$t_f = 85^\circ\text{F}$   
 0.020-in. TRIP ON NOSE  
 $I = 13.6868 \text{ g cm}^2$   
 0.002-sec INTERVAL BETWEEN EXPOSURES

Fig. 2. High-speed motion pictures of 10-deg half-angle cone model launched at 20-deg angle of attack

#### IV. DEVELOPMENT HISTORY AND PROBLEMS

The original launch system shown in Fig. 3 projected the models at 0-deg angle of attack only. Examination of the high-speed movies indicated that the models were being influenced by the bow shock of the launch tube

and would pitch or yaw as they passed through this shock. To correct this, the supporting piston (sabot) was extended to release the model upstream of the launch-tube bow shock. In addition, the air in the interior of

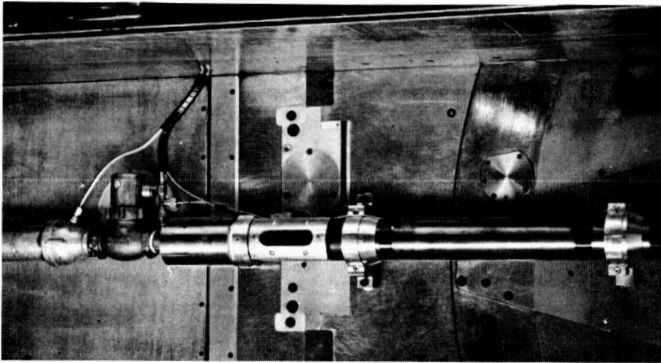


Fig. 3. Early installation of pneumatic launching assembly

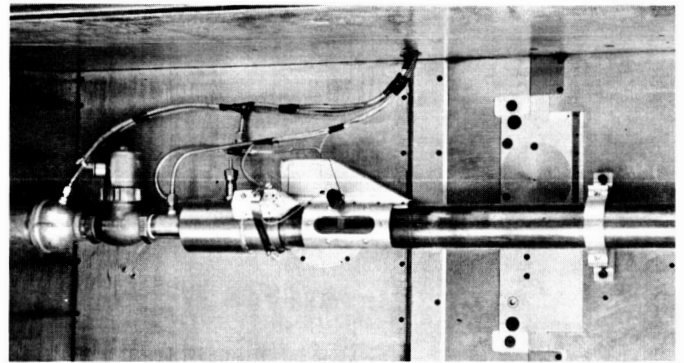


Fig. 4. Later developments of launching system, installation in supersonic facility

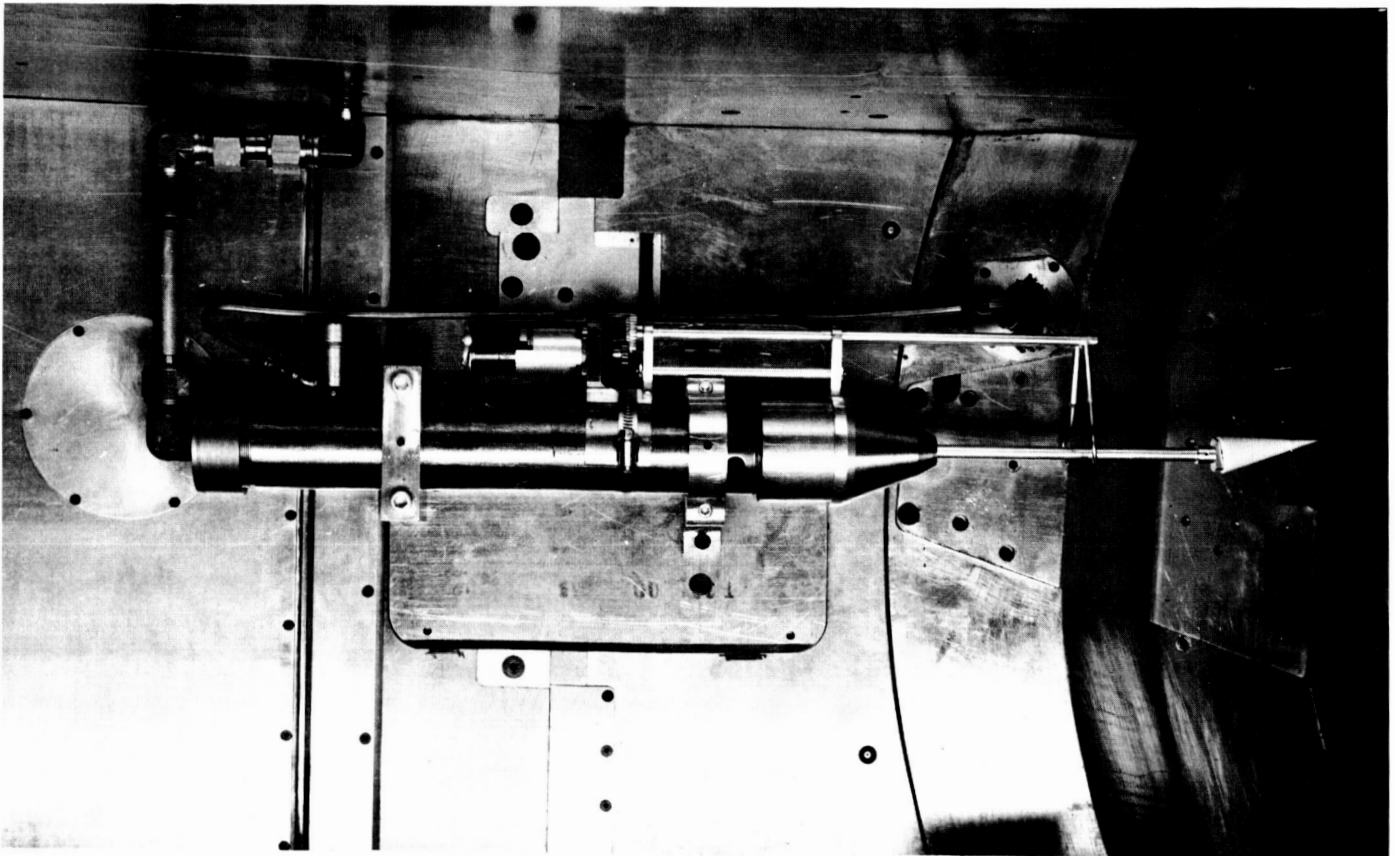
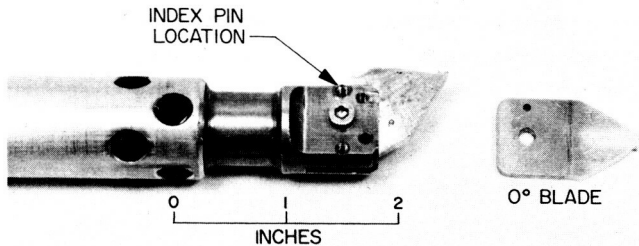


Fig. 5. Installation of launching system with model exposed to airstream

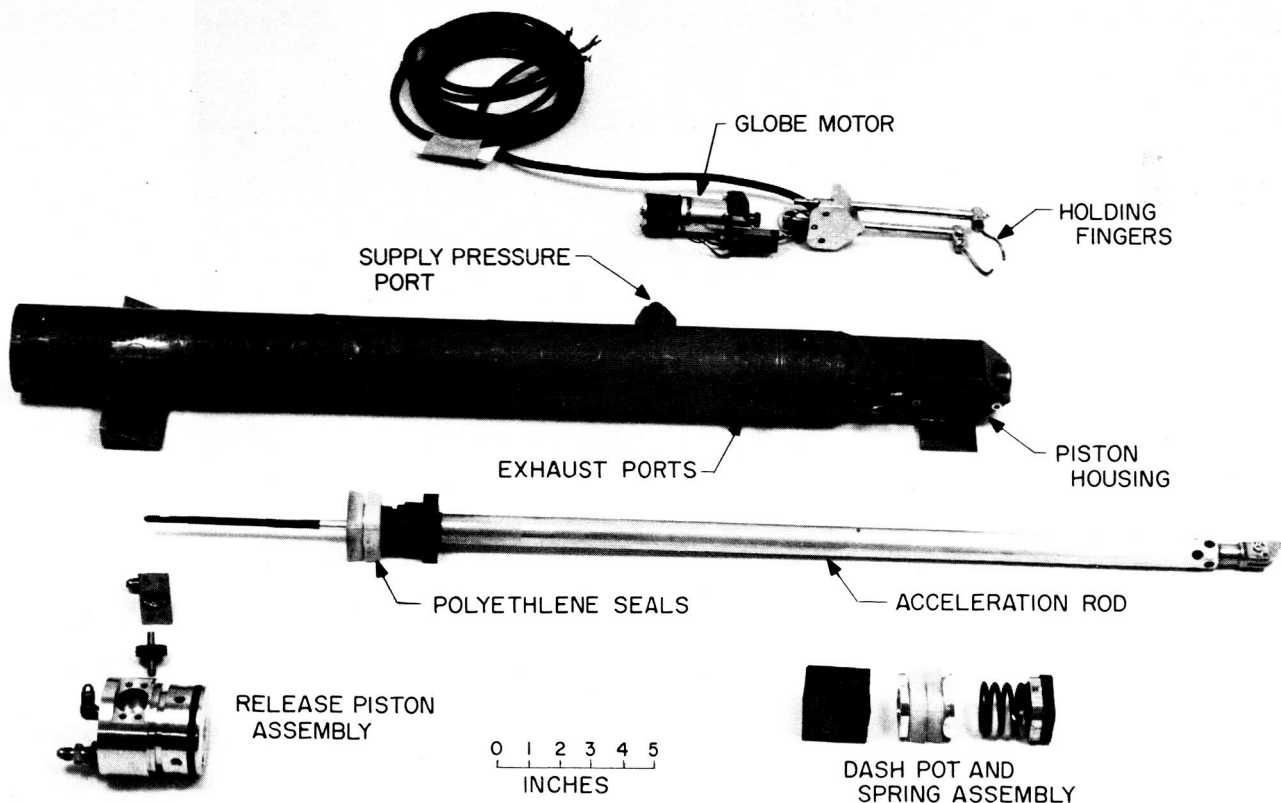
the tube could become resonant, and the models were usually blown off the support before launch. Figure 4 shows an illustration of a mechanical latch used to hold the model. The latch was released just before the piston was accelerated. This approach was abandoned in favor of supporting the model in the airstream, as shown in

Fig. 5. Also, modifications were made in the method of releasing the piston. (An air-actuated auxiliary piston was used.) Development was concentrated next on the support and release of the models at discrete angles of attack.

The difficulties encountered in supporting the model at angle of attack were shock interference from adjacent tunnel structure, and a force couple during the acceleration phase. Both of these problems were solved with the use of a triangular-shaped blade, placed vertically on the rod (Fig. 6). This type of support gave maximum side-load resistance to shock waves from the splitter-plate leading edge (a centerline section from the tunnel floor to the ceiling, running the length of the contraction section). The same support also resisted the vertical-force couple since the star-shaped point tended to bite into the plastic model and hold it in place. The triangular-blade supports shown in Fig. 6 illustrate the method by which the various angles of attack were set from 0 to 30 deg. While this method of model support was



**Fig. 6. Triangular-shaped blade support for cone models**



**Fig. 7. Components of pneumatic launcher**



adequate for the cone models, other model shapes may require further support development.

To prevent the acceleration rod from rotating during the launching action, the launch tube was fabricated from square tubing. The piston was then made to seal by vacuum-forming square cups of polyethylene sheet plastic. The various sections of the launch tube are shown in Fig. 7. A combination of a pneumatic dash pot and a coiled spring were used to stop the acceleration rod. The drive-piston packing sealed off the exhaust ports near the end of the stroke, and back pressure developed. Any follow-through was taken up by the coiled spring. This system was effective in decelerating the piston and rod assembly within 1 in., from a velocity of 100 ft/sec to zero (which has been the maximum

deceleration required to date for the models tested). Bench calibrations were performed to evaluate the system's repeatability at various piston-supply pressures. The setup is shown in Fig. 8. It consists of two photomultiplier tubes, light sources, and an oscilloscope. The velocities were computed from the time that it took the rod to travel through the last 4 in. before deceleration, and were recorded by the oscilloscope. The plotted data of supply pressure vs velocity are shown in Fig. 9, with an insert of a typical trace from the oscilloscope. From this information, it was possible to predict the pressures required to project the models at desired velocities. A less accurate approach to predicting the required pressure is working backwards from the equations of motion, Section VIII (Eq. 3), using the model's velocity ( $V_m$ ) in the equation

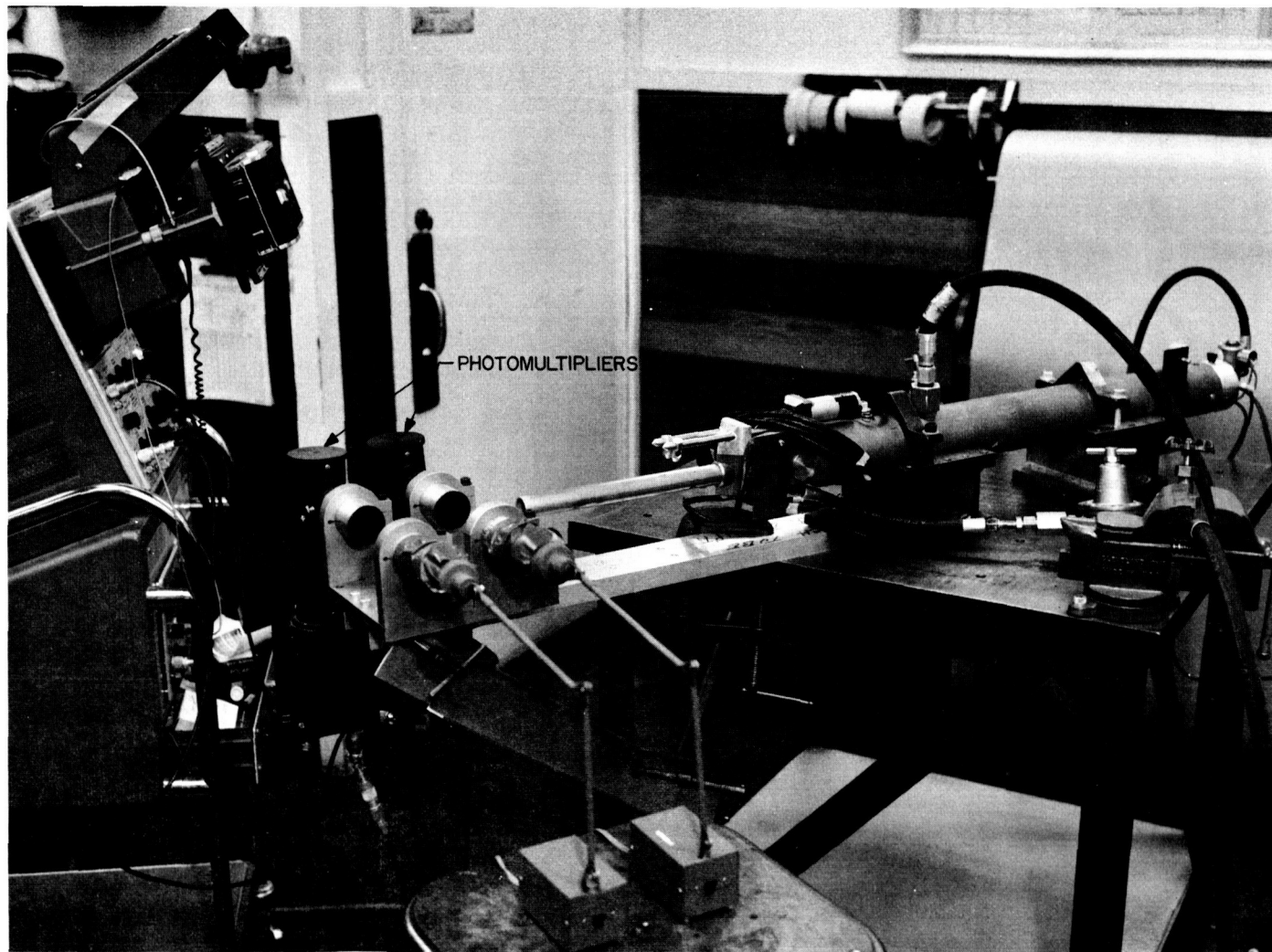


Fig. 8. Bench calibration setup

$$P = \frac{V_m^2 (m + m_1)}{2 SA_1}$$

As this method does not take into consideration the friction of the system, the first method is more applicable.

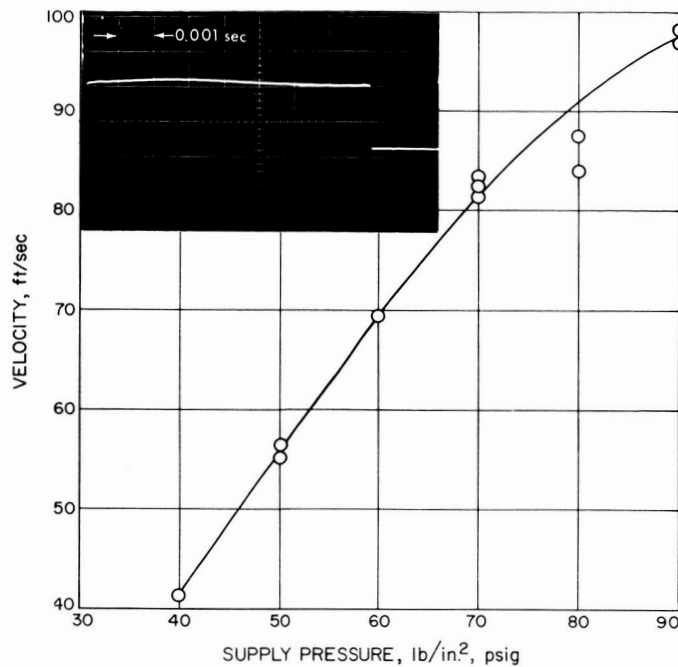


Fig. 9. Plot of velocity vs chamber pressure for launcher

## V. FUTURE DESIGN IMPROVEMENTS

In order to utilize the tunnel more efficiently, it is planned to install more than one launch assembly at a time, allowing two or more launches per tunnel entry. This will open up new approaches to the fabrication of a more elaborate system, such as two or more piston sections powered from a common supply tank, a pneumatically operated model clamp rather than the globe-

motor system now being used, a molded launch-pad for high alphas and special shapes (currently under development) and the development of a launching system for the hypersonic facility based on the knowledge gained from the development in the supersonic tunnel. Here, the exposed model, as well as the launching assembly, will have to be cooled.



## VI. MODEL CONSTRUCTION TECHNIQUES

Most all of the models in the early stages of free-flight testing were made of molded "polyurethane foam." For the wire-release method (Ref. 1) this was satisfactory; however, the construction was time-consuming and the dimensional stability of the foam varied with the weather conditions at the time of molding. Polyurethane-foam shapes were tried during the first attempts to launch models with the pneumatic launcher, but were discarded in favor of injection-molded polystyrene models. The early models of foam would break apart when subjected

to the launch-acceleration loads. Polystyrene was selected because of its excellent molding and impact properties. By experiment, it was found that models could be molded with wall thicknesses as thin as 0.020 in., which, when compared with a polyurethane-foam model of the same shape, had half the mass (before ballast was added). Another advantage of the injection molding process was the time saved. Models with excellent dimensional stability could be produced at the rate of approximately twenty per hour.

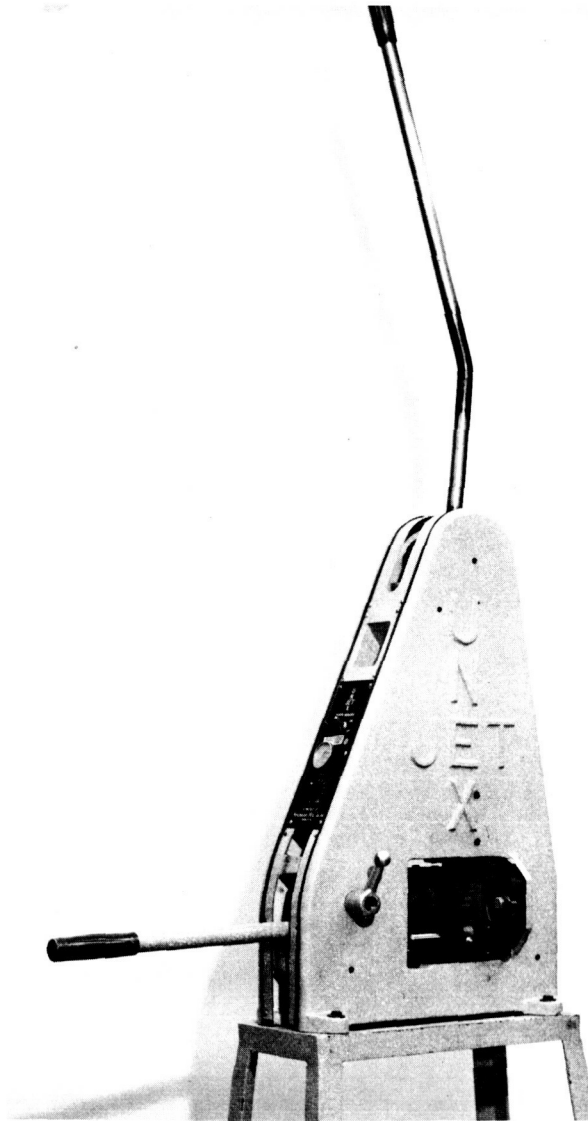


Fig. 10. Injection molding press

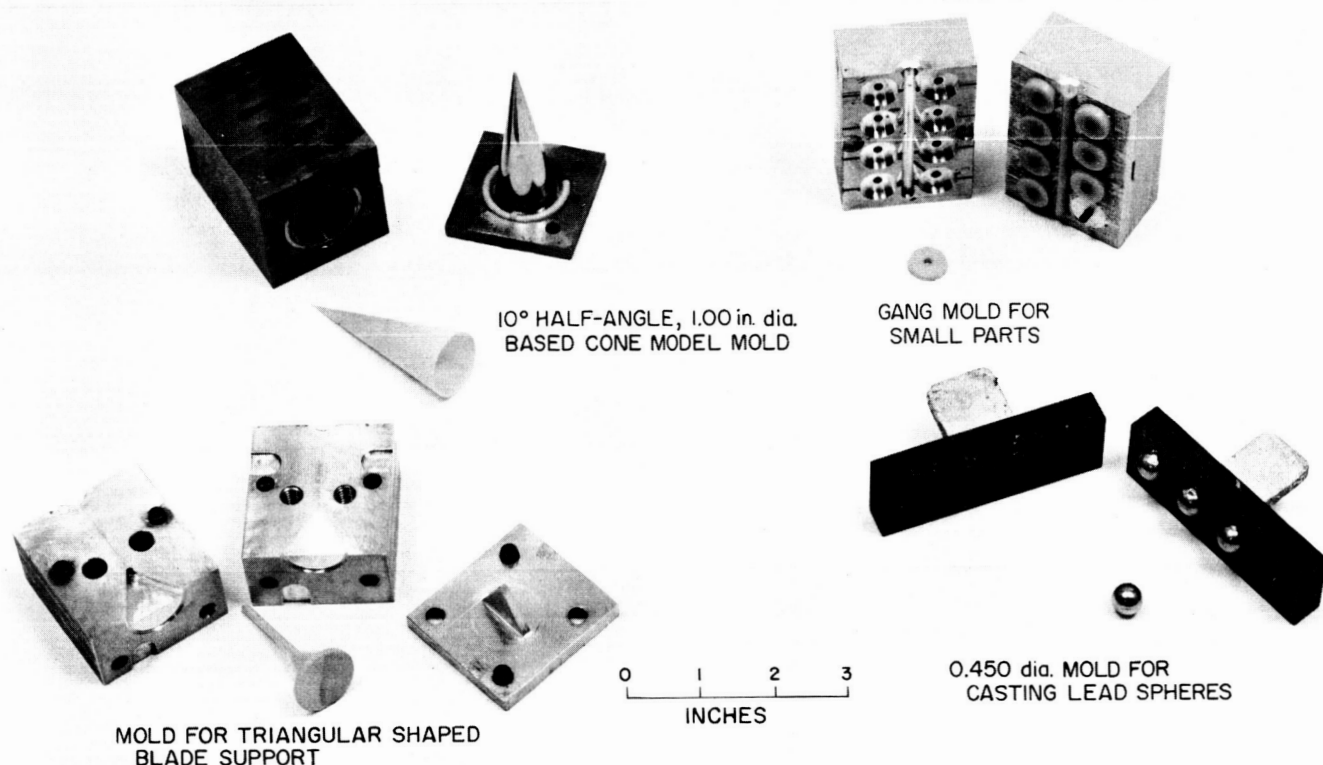


Fig. 11. Model mold of 10-deg half-angle 1.00-in. base diameter cone

The injection-molding press shown in Fig. 10 is a small hand-operated press used principally for sample runs or small experimental jobs. It will inject up to  $\frac{3}{4}$  oz of polystyrene per cycle, which is satisfactory for the present size of models being tested. Figure 11 shows the various molding dies required for one model, and Fig. 12 the completed model with a section removed to show the assembly.

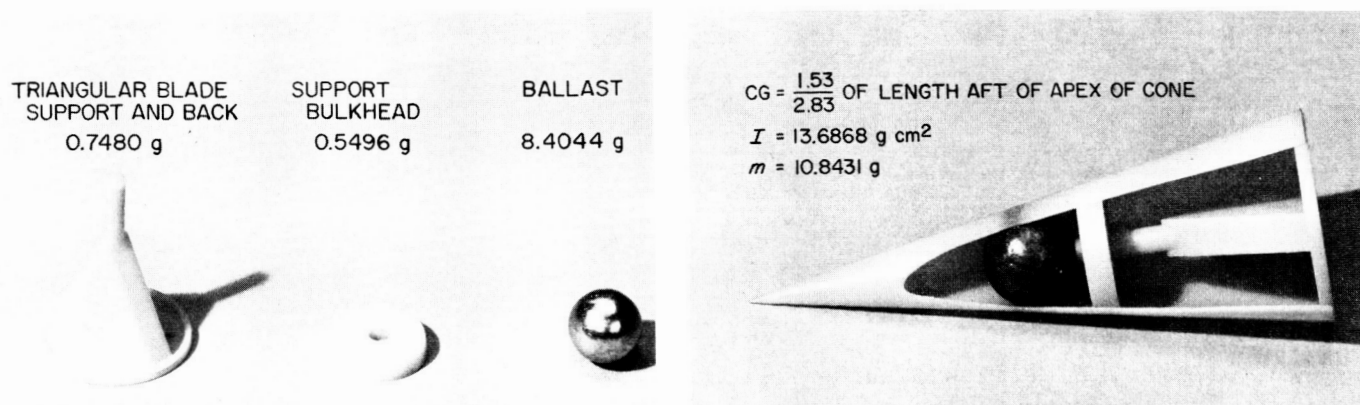


Fig. 12. Cutaway view of assembled 10-deg half-angle cone model

## VII. MOMENT-OF-INERTIA AND CENTER-OF-GRAVITY MEASUREMENTS

Determining the dynamic and static stability of a model in free flight requires exact measurements of the moment of inertia and center of gravity of the model. The two instrument assemblies used to make these measurements (Figs. 13 and 14) will be described separately.

### A. Moment of Inertia

The instrument package is composed of a wire and model support, light source, photo cell, electronic frequency divider, and a Beckman counter. The sensitivity of the package for measuring the period of a sample is

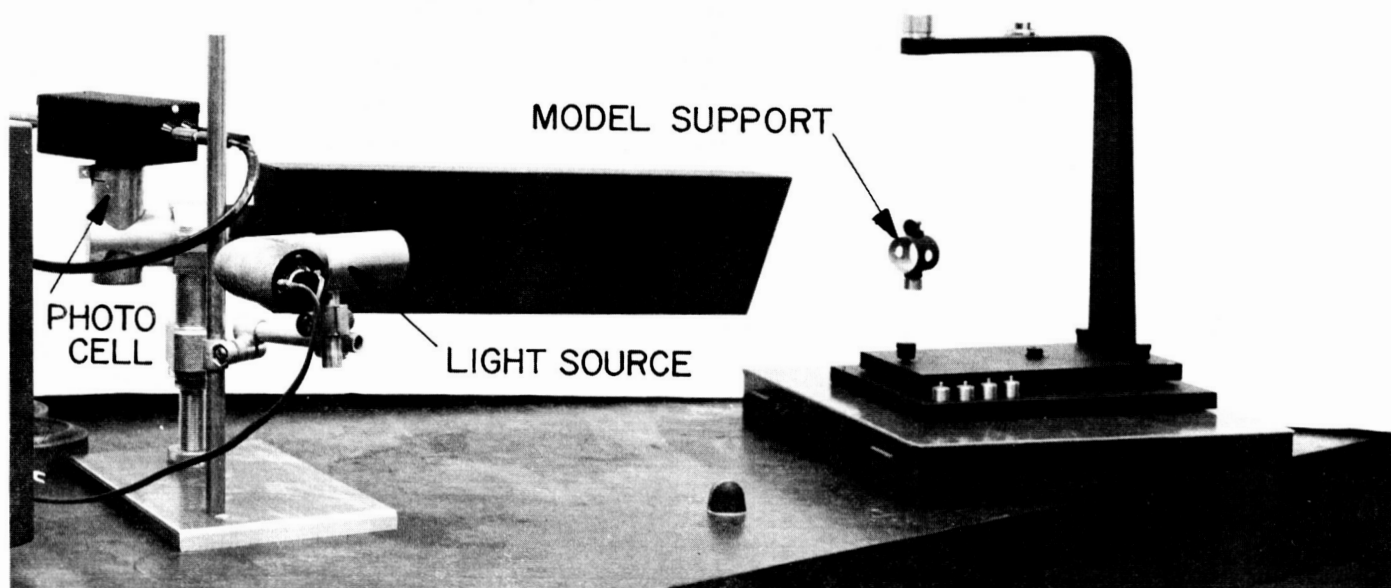
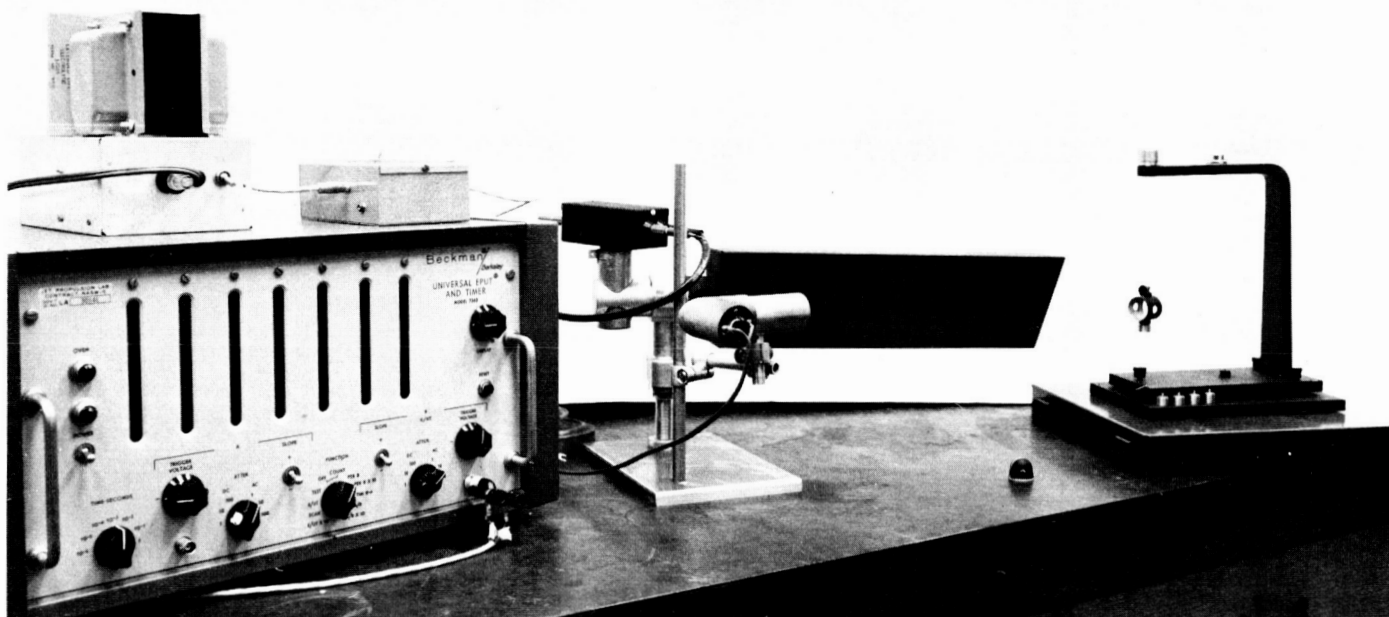


Fig. 13. Instrument for measuring the moment of inertia

$\pm 2 \times 10^{-4}$  sec. When a mass is large, 10 g and above, the viscous effect of the surrounding air has negligible effect on the period, whereas for samples where the mass is less than 1 g, measurements should be taken in a vacuum.

Calibration is accomplished by inserting precision discs, for which the moments of inertia have been calculated, into the model holders and recording their periods. A sample of the plotted values of  $I$  vs  $t^2$  is shown in Fig. 15. The model to be measured is then placed in the holding fixtures such that the line of action of the wire passes through the center of gravity. The period is then recorded. (At least five readings are taken to establish a true period.) This is squared, and the moment of inertia may be read directly from the calibration plot.

The method discussed above is used when there are a large number of models that have a wide variation in their moments of inertia. Another method is used for a group of models where the shape and mass of each is nearly the same. Record the period of a representative model. Then produce a calibrating disc that has a period

that nearly matches the period of the model and has a shape for which the moment of inertia can be calculated. " $I$ " can then be computed from the equation

$$I_m = I_c \left[ \frac{t_{m+f}^2 - t_f^2}{t_{c+f}^2 - t_f^2} \right]$$

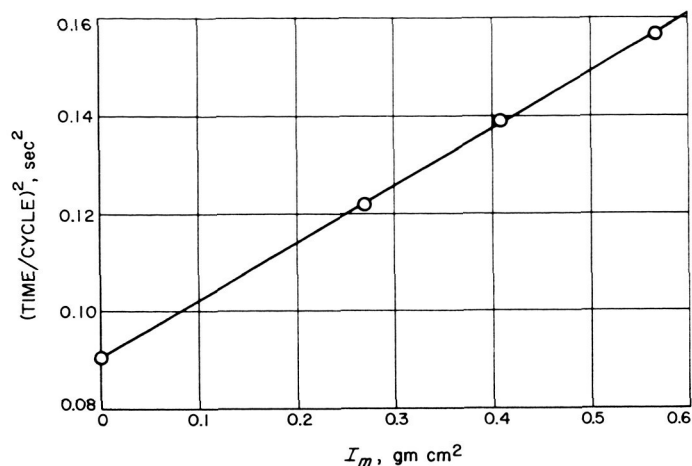


Fig. 15. Plot of  $I$  vs  $t^2$

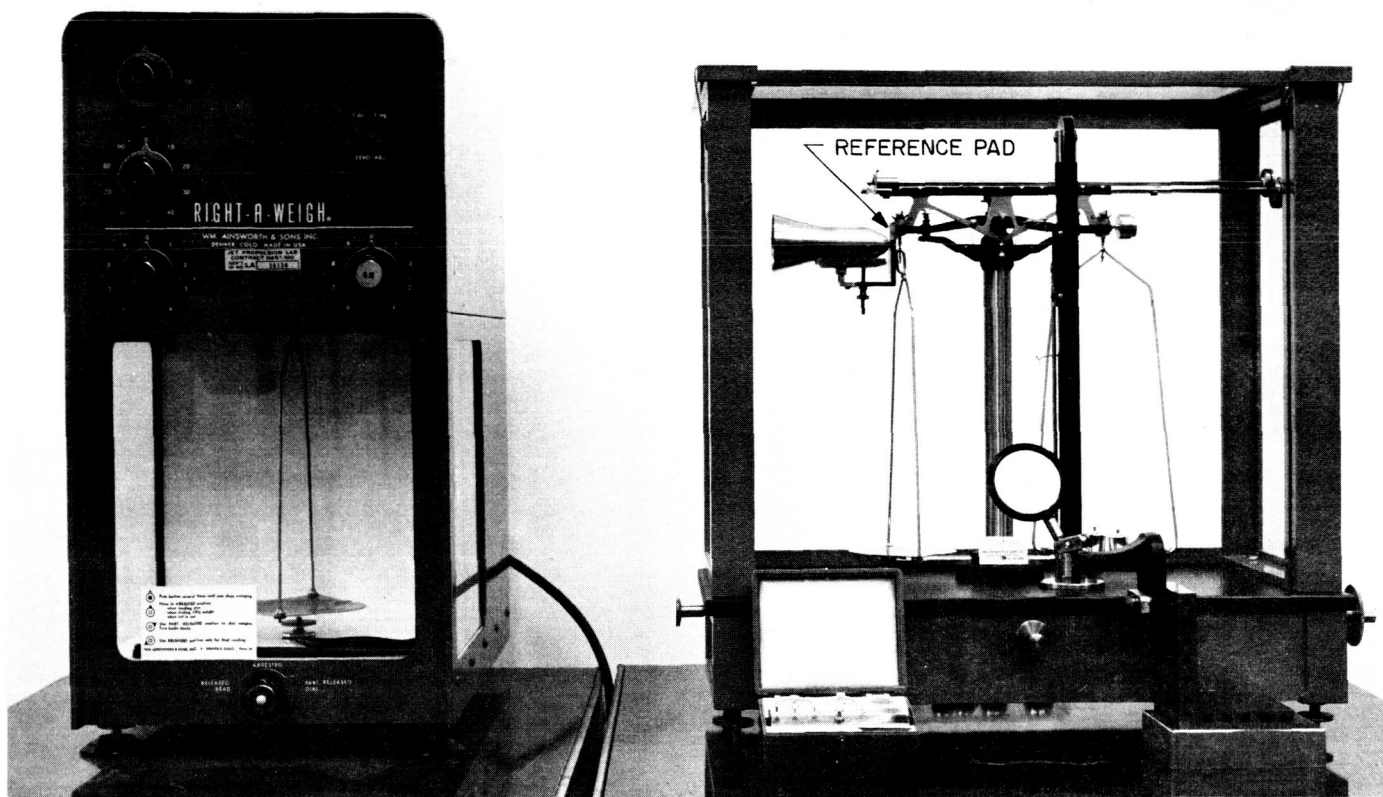


Fig. 14. Analytical balances for locating the center of gravity

For cases where the period of the holding fixture is small compared with that of the irregular shape, a simple ratio of the periods is adequate

$$I_m = I_c \left[ \frac{t_{m+f}^2}{t_{c+f}^2} \right]$$

Calculations of the moment of inertia can be made with accuracies to 0.4% when care is taken to be sure that the recorded period is valid; that is, the value has repeated several times without deviation.

### B. Center of Gravity

The instrument for locating the center of gravity consists of two analytical balances capable of measuring to 0.1 mg. One balance is used to measure the mass ( $m$ ) only, while the left-hand beam of the other has been altered to provide a reference pad, and platform to support the model. The accuracy to which the balance point could be determined was greatly improved by the addition of a microscope for viewing the swing of the pointer. (The microscope is not shown in Fig. 14.) Precision ball bearings ranging in diameter from 0.250 in. (1.0469 g) to 1.00 in. (65.6900 g) were used to calibrate the system. Five measurements of each sphere indicated that the instrument is capable of locating the center of gravity to  $\pm 0.0005$  in. The equation used to reduce the two mass measurements to a distance (Fig. 16) is

$$L_3 = L_2 \left( \frac{m_2}{m} \right) - L_1$$

A plot indicating the accuracy to which measurements were made is shown in Fig. 17.

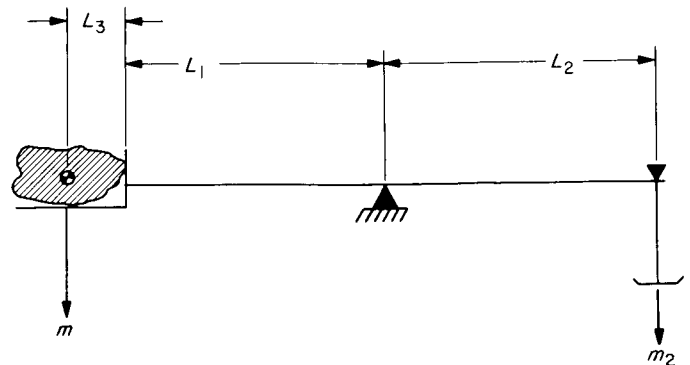


Fig. 16. Schematic of center-of-gravity measuring system

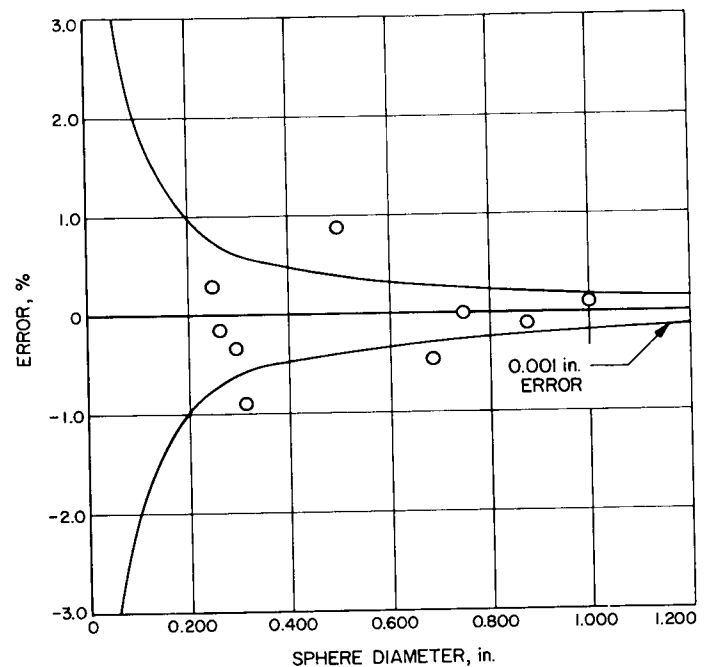


Fig. 17. Plot showing accuracy of center-of-gravity measurements

## VIII. APPROXIMATE EQUATIONS OF MOTION

In order to design suitable models, it is necessary to establish the probable motion of the models in free flight. Assuming linear aerodynamics, small angular oscillations, and a constant dynamic pressure (this usually varies less than 5%) the equations of motion are

$$m \ddot{S} - C_D q A = 0$$

$$I \ddot{\alpha} + M_D \dot{\alpha} + M_{\alpha} \alpha = 0$$

Solutions to these equations yield the following equations, which are useful in designing models for free-flight testing in the wind tunnel:

- (1) Model acceleration

$$a = \frac{q C_D A}{W} g$$

- (2) Time to travel distance S

$$t = \left( \frac{2 S m}{q C_D A} \right)^{1/2}$$

- (3) Model velocity at distance S

$$V_m = \left( \frac{2 S q C_D A}{m} \right)^{1/2}$$

- (4) Number of complete oscillation cycles in distance S

$$N = \frac{1}{\pi} \left( \frac{C_{m_a}}{C_D} S \frac{d m}{2 I} \right)^{1/2}$$

- (5) Oscillation frequency

$$f = \frac{1}{2\pi} \left( \frac{C_{m_a} A d q}{I} \right)^{1/2}$$

- (6) Decay in amplitude of oscillation due to dynamic damping contribution

$$\frac{\alpha_t}{\alpha_0} = \exp \left( \frac{-M_D}{2I} t \right)$$

where

$$M_D = (C_{m_q} + C_{m_{\dot{\alpha}}}) q \frac{A d^2}{V}$$

## IX. SUMMARY

The basic development of a pneumatic launcher is completed for use in the supersonic facility; however, unique problems will be encountered when a launcher is fabricated for the hypersonic facility. Although the information presented in this Report represents the early stages of a new technique in free-flight testing, there are many possibilities yet to be explored, such as dual flights of models launched from a single system, or by two launchers actuated simultaneously for separation studies

between two bodies; spin stabilized releases; and cold-wall studies. It is the intent of this Report to help those planning to fabricate such a system to benefit from the experience at JPL.

Expendable models are rather costly if machined, because of the thin walls required (in the case of cone models), whereas the use of injection molding has

reduced this cost approximately 85%. Some of the advantages of plastic models over metal are: (1) the consistency of the dimensions between models, (2) the time saved in construction, (3) the lowered risk of damage to tunnel structures, and (4) greater latitude of  $m$  and  $I$ .

The measurements of mass, moment of inertia, and center of gravity of the models to accuracies sufficient to acquire dynamic stability data have contributed to making possible the techniques of free-flight testing in a conventional wind tunnel.

## NOMENCLATURE

$a$	model acceleration
$A$	model reference area
$A_1$	area of piston
$C_D$	model drag coefficient = drag/ $qA$
$C_{m_a}$	model pitch-moment slope coefficient = $M_a/qAd$
$C_{m_q} + C_{m_a}$	pitch damping coefficient
$d$	model reference length
$f$	oscillation frequency
$g$	acceleration due to gravity
$I$	total moment of inertia of spherical model about its center
$I_c$	moment of inertia of calibration disc
$I_m$	moment of inertia, irregular shape (model)
$L_1$	fixed distance from fulcrum to $m_2$ pan (inches)
$L_2$	fixed distance from reference to fulcrum (inches)
$L_3$	distance from reference plane to center of gravity (inches)
$m$	mass of model
$m_1$	mass of piston assembly
$m_2$	mass of balancing weights
$M$	Mach number
$M_D$	pitch damping
$M_a$	pitch moment slope/radian
$N$	oscillation cycles
$P$	launch tube supply pressure
$q$	freestream dynamic pressure, $\frac{1}{2}\rho V^2$
$S$	model or piston travel

$t$	time
$t_{m+f}$	period of irregular shape plus holding fixture
$t_{c+f}$	period of calibration disc plus holding fixture
$t_f$	period of holding fixture
$V$	tunnel freestream velocity
$V_m$	model velocity
$W$	weight of model = $mg$
$\alpha$	angle of attack
$\alpha_t$	amplitude of oscillation at time $t$
$\alpha_0$	amplitude of oscillation at $t = 0$
$\rho$	freestream air density

## REFERENCES

1. Dayman, B., *Simplified Free Flight Testing in a Conventional Wind Tunnel*, Technical Report No. 32-346, Jet Propulsion Laboratory, Pasadena, California, October 1962.
2. Dayman, B., *Optical Free Flight Wake Studies*, Technical Report No. 32-364, Jet Propulsion Laboratory, Pasadena, California, November 1962.
3. Jaffe, P., and Prislín, R. H., "Effect of Boundary Layer Transition on Dynamic Stability Over Large Amplitudes of Oscillation," AIAA Paper No. 64-427, June, 1964.



### **ACKNOWLEDGMENTS**

The development of the pneumatic launcher could not have been accomplished without the ingenuity of the technical groups involved. Their imagination and patient approach to the problems of model construction, model release, and launcher construction were primary factors for the early success of this free-flight testing technique. The assistance of Don Kirk of the NASA Ames Research Center in the measurements of moment of inertia and center of gravity is gratefully acknowledged.